

# PARAMETRIC X-RAYS AT FAST \*

Tanaji Sen<sup>†</sup>, Fermi National Laboratory, Batavia, IL 60510

## Abstract

We discuss the generation of parametric X-rays in the photoinjector at the new FAST facility at Fermilab. Detailed calculations of the intensity spectrum, energy and angular widths and spectral brilliance with a diamond crystal are presented. We also report on expected results with PXR generated while the beam is channeling. A new goniometer with several ports could allow the simultaneous detection of PXR at multiple energies. The low emittance electron beam makes this facility a promising source for creating brilliant PXR emission.

## INTRODUCTION

The passage of MeV scale electron beams through a crystal can produce hard X-rays via many processes including channeling radiation (CR) and parametric X-rays (PXR). PXR emission is understood as the scattering of the virtual photons associated with the electron beam off the atomic electrons in the crystal [1]. Compared to CR, PXR has the advantages of being tunable by rotating the crystal, lower linewidth and cleaner separation from background bremsstrahlung, albeit at the expense of a lower photon yield. At the new FAST (Fermilab Accelerator Science and Technology) facility, experiments to produce CR with 40-50 MeV electrons are about to begin [2]. Since PXR can also be produced using the same beam and the same crystal, we also plan to perform PXR experiments after the initial CR experimental run. In this paper, we present calculations of the expected PXR angular spectrum, yield and spectral brilliance, first in dedicated experiments and then while the crystal is aligned for channeling. We also discuss the flexibility to simultaneously produce PXR emission at several different energies with a new goniometer under construction.

## PXR SPECTRUM

The X-ray energy emitted by the PXR process while an electron traverses a crystal is given by

$$E_X(\theta_B) \equiv \hbar\omega_B = \hbar c \frac{g \sin(\theta_B + \alpha)}{2 \sin^2((\theta_D + \alpha)/2)} \quad (1)$$

where  $g = 2\pi/d$ ,  $d$  is the lattice spacing,  $\theta_B$  is the angle (Bragg angle) of the beam direction with the crystal plane,  $\alpha$  is the angle of the electron with the central electron beam direction, and  $\theta_D$  is the observation angle of the emitted radiation with the beam direction. Specular reflection occurs at  $\theta_D = 2\theta_B$ . The photon energy is independent of beam energy (for relativistic beams) and can be changed by rotating the crystal with respect to the beam direction.

\* Fermilab is operated by Fermi Research Alliance LLC under DOE contract No. DE-AC02CH11359

<sup>†</sup> tsen@fnal.gov

## Line Broadening

The PXR intensity spectrum (see e.g. [3]) predicts a delta function spectrum at integer multiples  $m\omega_B$  of the Bragg frequency. In practice, there are several mechanisms which broaden the frequency of each line in the spectral distribution. It is important to keep the linewidth as narrow as possible, which increases the spectral brilliance and monochromatic X-rays are also required in many applications. Geometric effects and multiple scattering are the dominant contributors to the PXR linewidth. The geometric sources include effects from a spread in electron angles impinging on the crystal planes as well as a spread in photon angles emitted from the crystal. It can be shown that the energy spread due to these geometric effects is (see [4] for a derivation)

$$\frac{\Delta E}{E} = \frac{1}{R} \left[ \left( \frac{\Delta x_{det} \sigma'_x}{2 \sin^2 \theta_B} \right)^2 + \cot^2 \theta_B \left\{ (\sigma_x \sin(\theta_B + \zeta))^2 + \left( t \frac{\sin 2\theta_B}{\sin(\theta_B + \zeta)} \right)^2 + (\Delta x_{det})^2 \right\} \right]^{1/2} \quad (2)$$

Here  $\Delta x_{det}$  is the width of the detector,  $\sigma_x, \sigma'_x$  are the rms electron beam size and divergence respectively,  $R$  is the distance from the crystal to the detector,  $t$  is the crystal thickness, and  $\zeta$  is the angle between the PXR plane and the crystal surface. Bragg geometry corresponds to  $\zeta = 0$  while in Laue geometry  $\zeta = \pi/2$ . For typical beam and crystal parameters, the dominant contributions are from the beam spot size and the detector width (first and third terms within curly braces above) while the contributions from the beam divergence and crystal thickness are significantly smaller.

A Monte-Carlo simulation is often used to estimate the effect of multiple scattering on the energy spread. However, this contribution can also be calculated analytically from the differential angular spectrum. The multiple scattering weighted distribution function in  $\theta_x$  (angular horizontal deviation from  $2\theta_B$ ) is [4]

$$\left( \frac{dN}{d\theta_x} \right)_{MS} = \mathcal{A} \int \int \int \frac{dz d\phi_x d\theta_y}{E_X(\theta_x + \phi_x) [\hat{n} \cdot \hat{v}] \sigma'_x(z)} \exp \left[ - \frac{z}{L_a |\hat{n} \cdot \hat{\Omega}|} - \frac{\phi_x^2}{2\sigma_x'^2} - \frac{\theta_x^2 \cos^2 2\theta_B + \theta_y^2}{[\theta_x^2 + \theta_y^2 + \theta_{ph}^2]^2} \right] \quad (3)$$

Here  $\hat{n}$  is the unit normal to the crystal surface,  $\hat{v}$  is the unit velocity vector,  $\hat{\Omega}$  is the unit vector along the outgoing PXR photon,  $z$  is the distance into the crystal, and  $\mathcal{A}$  includes all factors which do not depend on  $z, \theta_x, \theta_y$ . Within the integrand,  $E_X(\theta_x + \phi_x)$  denotes that the photon energy is evaluated at the angle  $(\theta_x + \phi_x)$ . The multiple scattering is included by the  $z$  dependent divergence which is given by  $\sigma'_x(z) = [(\sigma'_{x,0})^2 + (\sigma'_{MS}(z))^2]^{1/2}$  with  $\sigma'_{MS}(z) = (13.6/E_e) \sqrt{z/X_{rad}} [1 + 0.038 \log(z/X_{rad})]$ . Here  $E_e$  is the beam energy in MeV and  $X_{rad}$  is the radiation

Table 1: Bunch, macro-pulse and crystal parameters in FAST

Parameter	Value
Beam energy	50 [MeV]
Bunch charge	20 [pC]
Length of a macro-pulse	1 [ms]
Number of bunches/macro-pulse	2000
Macro-pulse repetition rate	5 [Hz]
Crystal, thickness	Diamond, 168 [ $\mu\text{m}$ ]

length in the crystal. From this weighted distribution, the average and rms width of the energy spectrum can be found from  $\langle E \rangle = \int E(dN/d\theta_x)_{MS}d\theta_x / \int (dN/d\theta_x)_{MS}d\theta_x$  and  $\sigma_{E,MS}^2 = \langle E^2 \rangle - \langle E \rangle^2$ . The expressions for the energy width have been checked against measured values of earlier experiments and found to be in good agreement [4].

### Spectral Brilliance

Expressed in conventional light source units, the average spectral brilliance can be written in terms of the averaged beam parameters and differential angular intensity spectrum per electron in a 0.1% bandwidth

$$B_{av} = \frac{I_{av}}{e} \frac{1}{\Delta E_X/E_X} \frac{dN}{d\Omega} \left\langle \frac{1}{\sigma_e^2} \right\rangle \times 10^{-15} \quad (4)$$

photons/s - (mm - mrad)<sup>2</sup> - 0.1%BW

where  $I_{av}$  is the average electron beam current,  $\Delta E_X/E_X$  is the relative energy width,  $dN/d\Omega$  is the angular yield in units of photons/(e<sup>-</sup>-sr), and  $\sigma_e$  is the electron beam spot size. Here  $\Delta E_X$  includes only the contributions to the spectral width from the crystal but does not depend on the detector parameters.

### PXR IN FAST

The goniometer in place for the channeling experiments at FAST has a view port at 90° which can be used to direct out PXR emission, thus the Bragg angle is set to be 45°. The relevant beam and crystal parameters are shown in Table 1. The bunch charge and the number of bunches per macro-pulse are lower than nominal operational values in FAST, mainly to avoid pulse pile up in the X-ray detector. Table 2 shows the line width and angular yield per electron from some low order reflection planes. The yield value includes the effect of attenuation over a 1m long path in air from the crystal to the detector, and also includes the angular broadening due to the detector angular resolution, the beam divergence and multiple scattering.

The crystal thickness is an important parameter that determines the PXR output. Figure 1 shows the impact of the crystal thickness on the angular yield and spectral brilliance for two different planes. The thickness is shown relative to the photon attenuation length  $L_a$ ; this length is larger for the (400) plane because of the higher photon energy. For the same absolute thickness, the angular yield with the (220)

Table 2: Photon yields and linewidths at a Bragg angle of 45° from PXR off some low order planes. Bragg geometry in all cases.  $L_{a,air}$  is the attenuation length in air.

Plane	$E_X$ [keV]	$\Delta E_X$ [eV]	$L_{a,air}$ [cm]	Yield [photons/e <sup>-</sup> -sr]
(1,1,1)	4.26	59	12.72	$3.7 \times 10^{-7}$
(2,2,0)	6.95	93	57.2	$9.9 \times 10^{-5}$
(4,0,0)	9.83	131	144.9	$8.8 \times 10^{-5}$

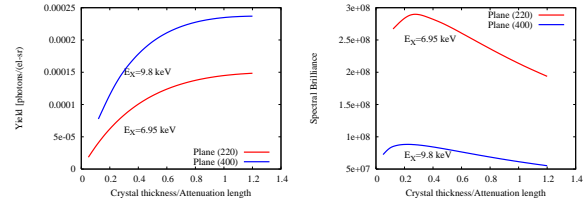


Figure 1: Left: Yield per electron per steradian as a function of the crystal thickness relative to  $L_a$  in the crystal for two planes. Right: Spectral brilliance as a function of the relative thickness for these planes.

plane is larger, but for the same relative crystal thickness the yield is higher with the (400) plane because the absolute thickness is larger. In both cases, the angular yield appears to saturate at a thickness of about  $1.2L_a$ . The spectral brilliance for the same relative crystal thickness is larger with the (2,2,0) plane because the average emittance over the crystal is smaller with a smaller absolute thickness. In both cases, the brilliance reaches a maximum around  $(0.2 - 0.3)L_a$ , and then falls quickly. These plots show that the optimum crystal thickness depends on whether the photon yield or the spectral brilliance is the object of interest.

### PXR WHILE CHANNELING

Under the right conditions an electron beam may emit PXR while being channeled and emitting CR [5]; this radiation is abbreviated as PXRC. PXRC may be emitted off allowed planes that intersect the channeling plane at some angle. The requirement that the PXRC be directed out at right angles to the beam direction while channeling parallel to the (1,1,0) plane, as is the case for the CR experiments at FAST, constrains the suitable planes for PXR emission. A geometrical analysis [4] had shown that theoretically six planes could be chosen, but most required some rotation of the crystal which would still maintain channeling. Only the (2,0,2) plane requires no further rotation for simultaneous observation of CR and PXR. Our considerations below are limited to this plane.

We used the expressions for the PXRC yields in [6] but modified them to include the effects of beam divergence [4]. The wave functions for channeling were calculated with a Mathematica program [7] significantly modified and corrected [8]. Fig. 2 shows the yields as functions of the photon emission angles  $\theta_x, \theta_y$  for PXR without channeling

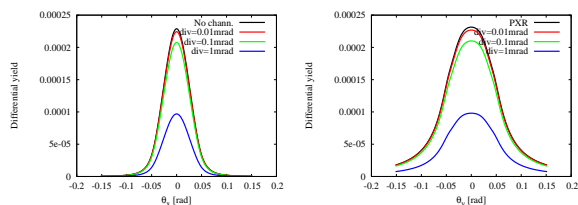


Figure 2: The differential yield as a function of the photon emission angle  $\theta_x$  (left) and  $\theta_y$  (right) without channeling and with channeling for three values of the initial beam divergence.

Table 3: Comparison of yield [units:  $\times 10^{-4}$  photons/(e<sup>-</sup>-sr)] and spectral brilliance (Sp. Br.) [units: photons/s-(mm-mrad)<sup>2</sup>- 0.1% BW] without and with channeling for three beam divergences ( $\sigma'$ ). Channeling plane: (1,1,0); angle  $\zeta = 60^\circ$ . The X-ray energy is 6.95keV and energy spread is 93 eV.

Plane	$\sigma'$ mrad	Yield		Sp. Br.	
		PXR / PXRC	PXR / PXRC	PXR / PXRC	PXR / PXRC
(2,0,2)	0.01	0.40 / 0.38	35.9 / 35.1		
	0.1	0.40 / 0.35	$2.1 \times 10^5$ / $1.9 \times 10^5$		
	1.0	0.40 / 0.16	$6.5 \times 10^8$ / $1.8 \times 10^8$		

and PXRC for three values of the beam divergence. It is clear that for very low beam divergence, the PXRC yields are close to those of PXR alone. Table 3 compares the spectral brilliance of PXR with PXRC. As expected, the brilliance is higher for the larger divergence or equivalently smaller beam size cases.

### NEW GONIOMETER

A new goniometer under construction, shown schematically in Fig. 3, will have multiple ports. These ports offer the opportunity of generating PXR at different Bragg angles and hence different energies, yields and spectral brilliance from those considered above. Here we consider PXR alone,

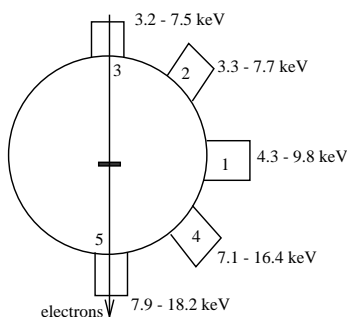


Figure 3: Schematic top view of a new goniometer with five labeled ports. The X-ray energies expected are shown, the range at each port represents different planes. Note: Ports 3 and 5 are at 45° to the horizontal.

Table 4: PXR photon energy and spectral brilliance (Sp. Br.) [units:  $\times 10^8$  photons/s-(mm-mrad)<sup>2</sup>- 0.1% BW] at ports 4 and 5 for different planes. The crystal thickness was 0.168mm.

Port	Plane 111		Plane 220	
	Energy	Sp. Br.	Energy	Sp. Br.
4	7.1	5.5	11.6	2.2
5	7.9	5.7	12.8	2.1
Port	Plane 311		Plane 400	
	Energy	Sp. Br.	Energy	Sp. Br.
4	13.6	0.59	16.4	0.59
5	15.1	0.57	18.2	0.56

without the constraints from channeling. Table 4 shows the spectral brilliance expected from ports 4 and 5, the ones corresponding to the smallest Bragg angles and highest yields. With the crystal thickness kept constant at 0.168 mm, the spectral brilliance is highest for the (111) plane at these ports. The X-ray energy for this plane is between 7-8 keV and the ratio of the crystal thickness to attenuation length is close to the optimal value of around 0.2, seen in Figure 1. For the higher order planes, the PXR energy increases but the spectral brilliance decreases. Especially for planes (3,1,1) and (4,0,0) the brilliance drops by an order of magnitude compared to the (1,1,1) plane. This is partly due to the small relative thickness and increasing the crystal thickness would also increase the brilliance. The choice of plane, i.e. crystal orientation, would then be determined by whether higher energy or higher brilliance is more desirable.

### CONCLUSIONS

We considered the prospect of generating PXR using diamond crystals with 50 MeV electron beams at the FAST facility. Using the 90° port of the goniometer installed for channeling allows a clear separation of PXR from the electron beam and background bremsstrahlung. PXR energies from low order planes are in the range 4 - 10 keV with energy widths of ~ 1%. PXR under channeling conditions was studied and the yield with quantum corrections from channeling was calculated. The highest yield is obtained with the lowest divergence, but higher brilliance favors the largest divergence. This PXRC emission makes possible simultaneous X-ray emission from channeling and PXR at 90° to each other. Finally, PXR emission with a new goniometer with five possible ports was studied. The range of energies now spans 3 - 18 keV. Use of this goniometer would open up the possibility of extracting PXR at multiple energies simultaneously.

**REFERENCES**

- [1] M.L. Ter-Mikaelian, *High energy electromagnetic processes in condensed media*, Wiley Interscience, New York (1972)
- [2] J. Hyun et al, this conference
- [3] P. Rullhusen et al, *Novel Radiation Sources using Relativistic Electrons*, World Scientific Publishing Co. (1998)
- [4] T. Sen and T. Seiss, FERMILAB-PUB-15-267-APC
- [5] R. Yabuki et al, Phys. Rev. B, **63**, 174112 (2001)
- [6] K.B. Korotchenko et al, JETP, **95**, 481 (2012)
- [7] B. Azadegan, Comp. Phys. Comm., **184**, 1064 (2013)
- [8] T. Sen and C. Lynn, Int. J. Mod. Phys. A, **29**, 1450179 (2014)